Journal of Neuroscience Research

Journal of Neuroscience Research 90:243–256 (2012)

Inhibition of Inflammation and Oxidative Stress by *Angelica dahuricae radix* Extract Decreases Apoptotic Cell Death and Improves Functional Recovery After Spinal Cord Injury

Youn Joo Moon,[1,2] Jee Youn Lee,[1,2] Myung Sook Oh,[3] Youngmi Kim Pak,[1,2,4] Kang-Sik Park,[2,4] Tae Hwan Oh,[1] and Tae Young Yune[1,2,5]*

[1]Age-Related and Brain Diseases Research Center, Kyung Hee University, Seoul, Korea
[2]Neurodegeneration Control Research Center, Kyung Hee University, Seoul, Korea
[3]Department of Oriental Pharmaceutical Science, College of Pharmacy, Kyung Hee University, Seoul, Korea
[4]Department of Physiology, School of Medicine, Kyung Hee University, Seoul, Korea
[5]Department of Biochemistry and Molecular Biology, School of Medicine, Kyung Hee University, Seoul, Korea

Inflammation and oxidative stress play major roles in the pathogenesis after spinal cord injury (SCI). Here, we examined the neuroprotective effects of *Angelica dahuricae radix* (ADR) extract after SCI. ADR extract significantly decreased the levels of proinflammatory factors such as tumor necrosis factor-α (TNF-α), interleukin-1β (IL-1β), interleukin-6 (IL-6), inducible nitric oxide synthase (iNOS), and cyclooxygenase-2 (COX-2) in a lipopolysaccharide (LPS)-activated microglial cell line, BV2 cells. ADR extract also significantly alleviated the level of reactive oxygen species in LPS-activated BV2 cells. To examine the neuroprotective effect of ADR extract after SCI, spinally injured rats were administered ADR extract orally at a dose of 100 mg/kg for 14 days. ADR extract treatment significantly reduced the levels of TNF-α, IL-1β, IL-6, iNOS, and COX-2. The levels of superoxide anion ($O_2 \cdot^-$) and protein nitration were also significantly decreased by ADR extract. In addition, ADR extract inhibited p38 mitogen-activated protein kinase activation and pronerve growth factor expression in microglia after SCI. Furthermore, ADR extract significantly inhibited caspase-3 activation following apoptotic cell death of neurons and oligodendrocytes, thereby improving functional recovery after injury. Thus, our data suggest that ADR extract provides neuroprotection by alleviating inflammation and oxidative stress and can be used as an orally administered therapeutic agent for acute SCI.

Key words: apoptosis; proinflammatory factors; microglia; neuroprotection; reactive oxygen species

Spinal cord injury (SCI) induces massive apoptotic cell death of neurons and oligodendrocytes, resulting in axonal degeneration and demyelination, thereby leading to spinal cord dysfunction (Liu et al., 1997; Springer et al., 1999; Lee et al., 2003; Yune et al., 2007). Inflammation and oxidative stress are major factors exacerbating the pathogenesis after SCI by inducing apoptosis of neurons and oligodendrocytes (Bao and Liu, 2002; Bareyre and Schwab, 2003; Lee et al., 2003; Yune et al., 2007, 2008). In particular, microglia play a pivotal role in inducing inflammatory responses and are believed to contribute to the neurodegenerative process by releasing both proinflammatory cytokines (Block and Hong, 2005) and reactive oxygen species (ROS; Min et al., 2003, 2004; Qin et al., 2004). After SCI, activated microglia also produce p38 mitogen-activated protein kinases (MAPK)-dependent pronerve growth factor (pro-NGF), which is known to be involved in apoptotic cell death of oligodendrocytes (Yune et al., 2007). Therefore, it is desirable to develop effective therapeutic interventions for preventing inflammation and oxidative stress via inhibition of microglial activation after SCI.

Angelica dahuricae radix (ADR), the dried root of *Angelica dahuricae* (Umbelliferae), is one of the most

Contract grant sponsor: Basic Science Research Program through the National Research Foundation of Korea (NRF); Contract grant number: 20100001758 (to S.R.C.); Contract grant sponsor: Brain Research Center of the 21st Century Frontier Research Program funded by the Ministry of Education, Science and Technology, Republic of Korea; Contract grant numbers: 2010K000824 and 2010K000833.

*Correspondence to: Tae Y. Yune, Department of Biochemistry and Molecular Biology, School of Medicine, Kyung Hee University, Seoul, Republic of Korea. E-mail: tyune@khu.ac.kr

Received 4 January 2011; Revised 19 May 2011; Accepted 10 June 2011

Published online 15 September 2011 in Wiley Online Library (wileyonlinelibrary.com). DOI: 10.1002/jnr.22734

common herbal remedies in Oriental medicine (Perry, 1980; Hsu et al., 1986) and has been used to counter harmful external influences on the skin, such as cold, heat, dampness, and dryness (Chevallier, 2001). ADR is also used as an antipyretic and analgesic for treatment of various symptoms such as acne, erythema, headache, sinusitis, colds, and flu (Wanger, 1999). Furthermore, ADR extract is known to exhibit liver protective activity, antimicrobial activity, antiinflammatory activity, and antimutagenic activity (Kim et al., 1991; Piao et al., 2004). Large numbers of chemical constituents such as coumarins and furanocoumarins (e.g., coumarin, scopoletin, isoimperatorin, imperatorin, oxypeucedanin, byakangelicol, and byakangelicin) have been identified from ADR extract (Saiki et al., 1971; Ketai et al., 2001). Among them, both isoimperatorin and imperatorin have been known to inhibit cyclooxygenase and lipoxygenase pathways of arachidonate metabolism in macrophages (Abad et al., 2001). Imperatorin has also been known to have inhibitory effect on concanavalin A-induced hepatitis in mice (Okamoto et al., 2001).

Recent evidence indicates that ADR extract has both antioxidant and antiinflammatory properties. For example, fluranocoumarins from ADR extract exhibit potent antioxidant activities in epithelial cells (Piao et al., 2004). The ethyl acetate extract of ADR inhibits LPS-induced expression of inflammatory mediators such as nitric oxide (NO), inducible nitric oxide synthase (iNOS), cyclooxygenase-2 (COX-2), and tumor necrosis factor-α (TNF-α) in macrophages by inhibiting mitogen-activated protein kinases (MAPKs) and IκB/NF-κB signal pathways (Kang et al., 2007). With these observations, we examined whether ADR extract may exert its neuroprotective effect by inhibiting microglial activation following inflammation and oxidative stress after SCI. Here, we found that ADR extract inhibited apoptosis by alleviating inflammatory responses and oxidative stress via inhibition of microglial activation, thereby improved functional recovery after SCI.

MATERIALS AND METHODS

Preparation of ADR Extract

ADR extract was prepared from dried roots of *Angelica dahurica* with 70% ethanol as described previously (Kim et al., 2001). The ethanol filtrate was evaporated in vacuo, and powdered ADR was stored at −20°C until use. As previous reported by Park et al. (2009), ADR extract contains various compounds such as byakangelicol (0.0687%), oxypeucedanin (0.0586%), imperatorin (0.0295%), phellopterin (0.0144%), and isoimperatorin (0.0149%) by HPLC/UV analysis.

Microglia Culture

The murine microglia (BV2) cell line (Blasi et al., 1990) was cultured in DMEM supplemented with 5% fetal bovine serum, 100 U/ml penicillin, and 100 g/ml streptomycin at 37°C in a humidified incubator under 5% CO_2. Before each experiment, cells (1×10^5 cells per well) were plated onto 24-well plates. On the next day, cells were pretreated with ADR extract (1, 10, and 50 μg/ml) for 30 min before LPS (100 ng/ml; *Escherichia coli* 0111:B4; Sigma, St. Louis, MO) treatment. Powdered ADR extract was dissolved in dimethylsulfoxide (DMSO) and then diluted in PBS (final concentration of DMSO 0.1%). For control, diluted DMSO (0.1%) without ADR extract was used.

Assays for ROS and NO Production

The ROS production was measured fluorometrically using the ROS-specific fluorescence dye dichlorodihydrofluorescein diacetate (DCF-DA; Molecular Probes, Eugene, OR) as described previously (Kim et al., 2007). NO production was also measured as described previously (Lee et al., 2004). Briefly, 100 μl culture medium was allowed to react with 100 μl Griess reagent (Sigma). The optical density was read at 540 nm in a microplate reader (Molecular Devices, Sunnyvale, CA) after 15 min. Cellular nitrite production was quantitated by subtracting the level of nitrite present in the media (in the absence of cells) from the total nitrite level. Nitrite concentrations were calculated from a standard curve derived from the reaction of sodium nitrite in fresh media.

SCI

Adult Sprague-Dawley rats (male; 230–250 g; Samtako) were subjected to moderate contusion injury (10 g, 25 mm) as described previously (Yune et al., 2007). For the sham-operated controls, animals underwent a T10 laminectomy without weight-drop injury. Surgical interventions and postoperative animal care were performed in accordance with the Guidelines and Polices for Rodent Survival Surgery provided by the Animal Care Committee of the Kyung Hee University.

ADR Extract Administration

Powdered ADR extract was suspended in sterile deionized water and administered orally at a dose of 100 mg/kg beginning 2 hr after SCI and then once per day for 2 weeks. Control groups were received equivolumetric administration of sterile deionized water at the corresponding times.

In Situ Detection of Superoxide Anion

The production of superoxide anion ($O_2{\cdot}^-$) after SCI was examined by using HEt dye (Invitrogen, Carlsbad, CA). HEt is oxidized to the fluorescent ethidium by $O_2{\cdot}^-$ (Carter et al., 1994; Kondo et al., 1997) and is considered an indicator of intracellular $O_2{\cdot}^-$ (Yune et al., 2004). Two hundred microliters of HEt (1 mg/ml in phosphate-buffered saline, pH 7.4) was injected intravenously 1 hr before the animals were killed. Animals were killed 4 hr after injury, and spinal cord sections were prepared. The fluorescence was assessed microscopically at excitation (Ex) = 355 nm and emission (Em) > 415 nm for HEt detection or at Ex = 510–550 nm and Em > 580 nm for Etd detection and photographed with an Olympus microscope with software accompanying the Cool Snap camera (Roper Scientific). For quantitative analysis of ethidium fluorescence, the area of tissue fluorescence in three coronal sections from each animal was analyzed in MetaMorph software (Molecular Devices, Sunnyvale, CA) as described previously (Yune et al., 2008).

RNA Isolation and RT-PCR

RNA isolation using Trizol reagent (Invitrogen) and cDNA synthesis were performed as described previously (Lee et al., 2003). The primers used for iNOS, COX-2, TNF-α, interleukin-1β (IL-1β), IL-6, and GAPDH were synthesized by Genotech (Daejeon, Korea). The sequences of the primers were 5′-CTC CAT GAC TCT CAG CAC AGA G-3′ (sense) and 5′-GCA CCG AAG ATA TCC TCA TGA T-3′ (antisense) for iNOS, 5′-CCA TGT CAA AAC CGT GGT GAA TG-3′ (sense) and 5′-ATG GGA GTT GGG CAG TCA TCA G-3′ (antisense) for COX-2, 5′-CCC AGA CCC TCA CAC TCA GAT-3′ (sense) and 5′-TTG TCC CTT GAA GAG AAC CTG-3′ (antisense) for TNF-α, 5′-GCA GCT ACC TAT GTC TTG CCC GTG-3′ (sense) and 5′-GTC GTT GCT TGT CTC TCC TTG TA-3′ for IL-1β, 5′-AAG TTT CTC TCC GCA AGA TAC TTC CAG CCA-3′ (sense) and 5′-AGG CAA ATT TCC TGG TTA TAT CCA GTT T-3′ (antisense) for IL-6, and 5′-TCC CTC AAG ATT GTC AGC AA-3′ (sense) and 5′-AGA TCC ACA ACG GAT ACA TT-3′ (antisense) for GAPDH, which was used as an internal control. Experiments were repeated three times, and the values obtained for the relative intensity were subjected to statistical analysis. The gels shown in figures are representative results from three separate experiments.

Western Blot

Whole lysates from spinal cord (1 cm) or BV2 cells were prepared with a lysis buffer containing 1% Nonidet P-40, 20 mM Tris, pH 8.0, 137 mM NaCl, 0.5 mM EDTA, 10% glycerol, 10 mM $Na_2P_2O_7$, 10 mM NaF, 1 μg/ml aprotinin, 10 μg/ml leupeptin, 1 mM sodium vanadate, and 1 mM PMSF. The protein concentration was determined by using a BCA assay kit (Pierce, Rockford, IL). Protein samples (40 μg each) were separated on SDS-PAGE and transferred to nitrocellulose membrane (Millipore, Billerica, MA). The membranes were blocked in 5% nonfat skim milk or 5% bovine serum albumin in TBS-T (0.1% Tween 20) for 1 hr at room temperature, followed by incubation with antibodies against β-tubulin (1:10,000; Sigma), iNOS (1:10,000; Transduction Laboratories, Lexington, KY), COX-2 (1:1,000; Cayman Chemicals, Ann Arbor, MI), phosphorylated p38MAPK (p-p38MAPK; 1:1,000; Cell Signaling Technology, Danvers, MA), cleaved caspase-3 (1:1,000; Cell Signaling Technology), and pro-NGF (1:1,000; Santa Cruz Biotechnology, Santa Cruz, CA). Tubulin was used as an internal control. Relative intensity of each band on Western blots was measured and analyzed by AlphaImager software (Alpha Innotech Corporation, San Leandro, CA). Background in films was subtracted from the optical density measurements. Experiments were repeated three times, and the values obtained for the relative intensity were subjected to statistical analysis. The gels shown in figures are representatives of results from three separate experiments.

Tissue Preparation

After SCI, animals were anesthetized with 4% chloral hydrate and perfused via cardiac puncture initially with 0.1 M PBS (pH 7.4) and subsequently with 4% paraformaldehyde in 0.1 M phosphate buffer. A 20-mm section of the spinal cord, centered at the lesion site, was dissected out, postfixed by immersion in the same fixative overnight, and placed in 30% sucrose in 0.1 M PBS. The segment was embedded in OCT for frozen sections as described previously (Yune et al., 2007). Frozen tissues were then cut at 10 or 20 μm on a cryostat (Leica CM1850).

TUNEL and Immunohistochemical Staining

One and five days after injury, serial spinal cord sections (10 μm thickness) were collected every 100 μm and processed for terminal deoxynucleotidyl transferase (TdT)-mediated deoxyuridine triphosphate-biotin nick end labeling (TUNEL) staining using an Apoptag in situ kit (Chemicon, Temecula, CA). Diaminobenzidine (DAB) substrate kit (Vector Laboratories, Burlingame, CA) was used as a substrate for peroxidase, and the sections were then counterstained with methyl green. Control sections were incubated in the absence of TdT enzyme. All TUNEL analyses were carried out by investigators who were blind to the experimental conditions. Quantitation of TUNEL-positive cells was accomplished by counting the number of cells labeled positively with a ×20 objective. In total, 40 sections for neurons in the gray matter (GM) at 1 day and in total 100 sections for oligodendrocytes in the white matter (WM) at 5 days after SCI were counted and averaged. Only those cells showing morphological features of nuclear condensation and/or compartmentalization only in the GM and the WM were counted as TUNEL positive. The tissue sections were also processed for immunohistochemistry with antibodies against nitrotyrosine (1:500; Millipore), p-p38MAPK (1:1,000; Cell Signaling Technology), cleaved caspase-3 (1:100; Cell Signaling Technology), OX-42 (1:100; Millipore), and CC1 (1:100; Millipore), a cell-type-specific marker for oligodendrocytes. For double labeling, fluorescein isothiocyanate (FITC)- or cyanin 3-conjugated secondary antibodies (Jackson Immunoresearch, West Grove, PA) was used. Also, nuclei were labeled with DAPI according to the protocol of the manufacturer (Invitrogen). In all controls, reaction to the substrate was absent if the primary antibody was omitted or if the primary antibody was replaced by a nonimmune, control antibody. Serial sections were also stained for histological analysis with cresyl violet acetate. For quantification of cleaved caspase-3-positive oligodendrocytes (cleaved caspase-3/CC1 double positive), serial transverse sections (10 μm thickness) were collected every 200 μm from 4,000 μm rostral to 4,000 μm caudal to the lesion site (n = 4, total 40 sections per animal). Cleaved caspase-3-positive oligodendrocytes in the WM in each section were counted and averaged.

Quantitation of the Proportion of Resting and Activated Microglia

Percentage of field analysis was used to provide a quantitative estimate (proportional) of changes in the activation state of microglia. Resting and activated microglia were classified and counted based on a previous report (Hains and Waxman, 2006; Yune et al., 2009). Briefly, with immunostaing by OX-42 antibody (Millipore), resting microglia displayed small, compact somata bearing long, thin, and ramified processes.

Activated microglia exhibited marked cellular hypertrophy and retraction of processes such that the process length was less than the diameter of the soma compartment. Quantitative analysis was performed by blinded observers. Cells were sampled only if the nucleus was visible within the plane of section and if cell profiles exhibited distinctly delineated borders (Hains and Waxman, 2006).

Behavioral Tests

To examine functional deficits after injury, behavioral analyses were performed by trained investigators who were blind to the experimental conditions. For testing of hindlimb locomotor function, open-field locomotion was evaluated by using the 21-point Basso-Beattie-Bresnahan (BBB) locomotion scale as described elsewhere (Basso et al., 1995). BBB is a 22-point scale (scores 0–21) that systematically and logically follows recovery of hindlimb function from a score of 0, indicative of no observed hindlimb movements, to a score of 21, representative of a normal ambulating rodent. The inclined plane test was performed via a method described previously (Rivlin and Tator, 1977). In brief, animals were tested in two positions (right side or left side up) on the testing apparatus (i.e., a board covered with a rubber mat containing horizontal ridges spaced 3 mm apart). The maximum angle at which a rat could maintain its position for 5 sec without falling was recorded for each position, and averaged to obtain a single score for each animal. Footprint analysis was performed as described elsewhere (de Medinaceli et al., 1982; Stirling et al., 2004). The animal's forepaws and hindpaws were dipped in red and blue dye (nontoxic), and the animal was then allowed to walk across a narrow box (1 m long and 7 cm wide). The footprints were scanned, and digitized images were analyzed.

Axon Staining and Counting

Rats from the vehicle- and ADR extract-treated groups were anesthetized at 38 days after injury, and frozen sections were prepared as described above. For quantitative analysis of axonal densities, serial coronal sections collected every 1 mm rostral and 3 mm caudal to the lesion site were stained with an antibody specific for 200-kDa neurofilament protein (NF200; 1:4,000; Sigma). Axonal densities were determined within preselected fields (40×40 μm, 1,600 μm^2) at specific sites within the vestibulospinal tract (VST) for NF200-positive axons as previously described (Yune et al., 2007). The location of these sites was carefully conserved from group to group by using anatomical landmarks and remaining axons were manually counted from each field. The number of axons in vehicle- or ADR extract-treated spinal cord was expressed as a percentage relative to that in sham control (100%).

Luxol Fast Blue Staining

To assess the loss of myelin, serial transverse cryosections (16 μm thickness) were stained with Luxol fast blue as previously described (Yune et al., 2007). In brief, the selected slides were incubated in 0.1% Luxol fast blue (Solvent Blue 38; Sigma) in acidified 95% ethanol overnight at 60°C. Differentiation was carried out with 0.05% lithium carbonate.

Assessment of Lesion Volume

The measurement of lesion volume using rats tested for behavioral analysis was performed as previously described (Yune et al., 2008). Serial longitudinal sections (10 μm) through the dorsoventral axis of the spinal cord were used to determine lesion volume. Every 50-μm section was stained with cresyl violet acetate and was studied via light microscopy. The rostrocaudal boundaries of the tissue damage were defined by the presence of inflammatory cells, loss of neurons, existence of degenerating neurons, and cyst formation. With a low-power (×1.25) objective, the lesion area was determined in MetaMorph software (Molecular Devices). Areas at each longitudinal level were determined, and the total lesion volume was derived by means of numerical integration of sequential areas.

Statistical Analysis

Data are presented as mean ± SD. Comparisons between vehicle- and ADR extract-treated groups were made by unpaired Student's *t*-test. Multiple comparisons between groups were performed by one-way ANOVA. Behavioral scores from BBB analysis and inclined plane tests were analyzed by repeated-measures ANOVA (time vs. treatment). Tukey's multiple comparison was used as post hoc analysis. Statistical significance was accepted at $P < 0.05$. All statistical analyses were performed in SPSS 15.0 (SPSS, Chicago, IL).

RESULTS

ADR Extract Inhibits the Expression of Proinflammatory Mediators in BV2 Microglial Cells Activated by LPS

ADR is known to inhibit the expression of proinflammatory mediators such as TNF-α, iNOS, and COX-2 in macrophages (Kang et al., 2007), so we hypothesized that ADR extract would exhibit antiinflammatory effects in microglia. We first determined the effect of ADR extract on the cell viability in BV2 cells by using the 3-(4,5-dimethyl-thiazol-2-yl)-2,5-diphenyl tetrazolium bromide (MTT) assay at 24 hr after LPS treatment (Kim et al., 2007). ADR extract at concentrations of 1, 10, and 50 μg/ml exhibited no cytotoxic effect on BV2 cells (data not shown). Next, to examine antiinflammatory effects of ADR extract, we employed an in vitro model of LPS-induced microglial activation in BV2 cells. BV2 cells were pretreated with ADR extract (1, 10, and 50 μg/ml) for 30 min and then treated with LPS (100 ng/ml). As shown in Figure 1, ADR extract treatment at the concentrations of 10 and 50 μg/ml significantly decreased LPS-induced mRNA levels of TNF-α and IL-1β (2 hr) and of IL-6, COX-2, and iNOS (24 hr) in BV2 cells (Fig. 1A,B). In addition, the protein expression of COX-2 and iNOS was also inhibited by ADR extract treatment at 24 hr after LPS treatment (10 and 50 μg/ml; Fig. 1C,D).

ADR Extract Decreases LPS-Induced NO and ROS Levels in BV2 Cells

Since furanocumarins isolated from ADR extract show a potent antioxidant activity in epithelial cells

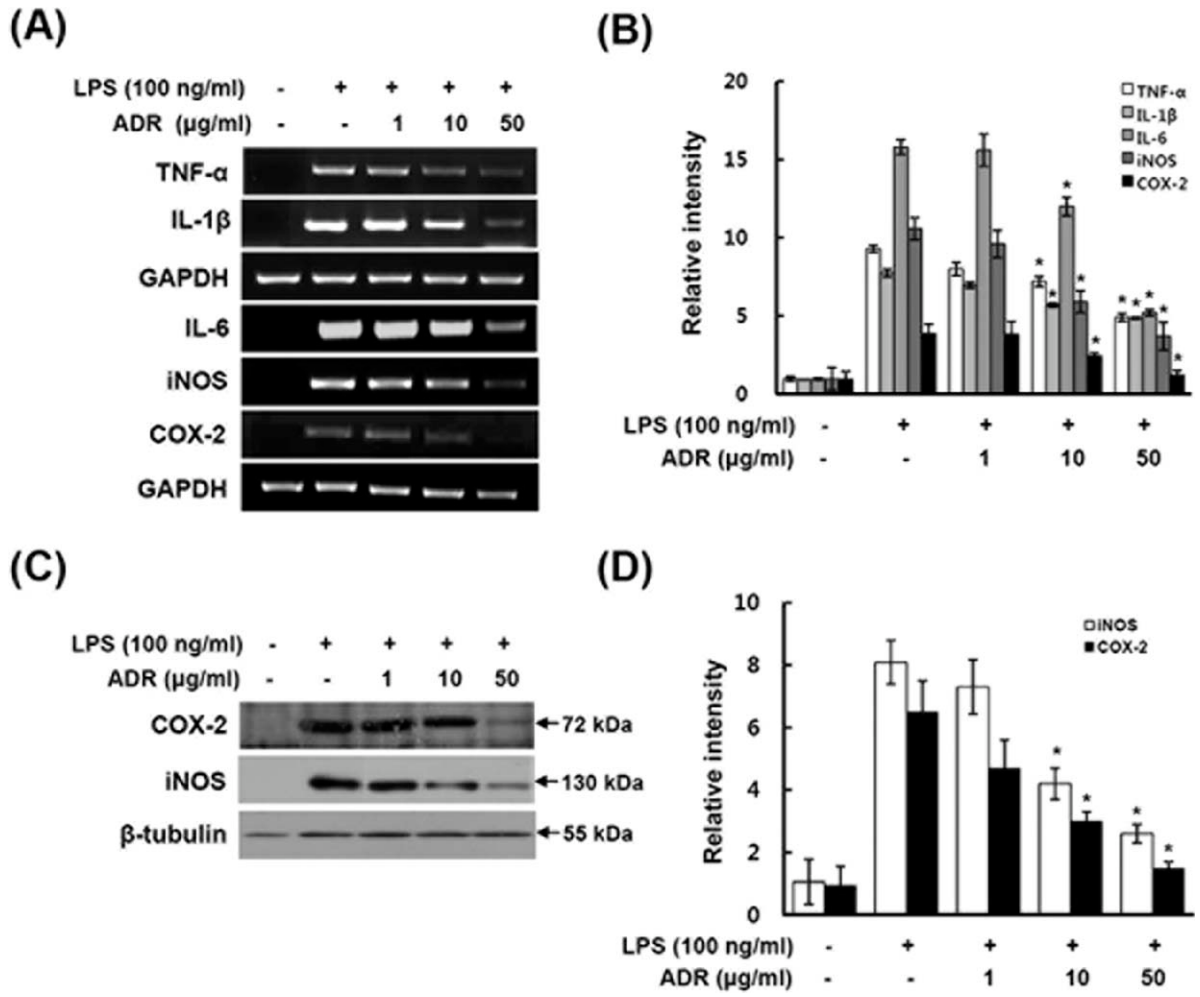

Fig. 1. ADR extract treatment inhibits the expression of proinflammatory cytokines and mediators in LPS-activated BV2 cells. BV2 cells were seeded in 24-well plates (1×10^5 cells/well) and treated with ADR extract (1, 10, and 50 μg/ml) 30 min before LPS (100 ng/ml) treatment. At indicated time points (2 hr for TNF-α and IL-1β and 24 hr for IL-6, COX-2, and iNOS), cells were harvested and processed for mRNA and total lysates isolation as described in Materials and Methods. RT-PCR (**A,B**) and Western blots (**C,D**) of proinflammatory cytokine and mediator expression in BV2 cells. The gels presented are representative of results from three separate experiments, and data are mean ± SD. $^{\star}P < 0.05$ vs. LPS-treated control.

(Piao et al., 2004), we expected that ADR extract would inhibit oxidative stress induced by LPS in microglia. We examined the effect of ADR extract on ROS level in LPS-activated BV2 cells using an ROS-specific fluorescent dye, DCF-DA. As shown in Figure 2A, the level of ROS was increased at 12 hr after LPS treatment. ADR extract treatment (50 μg/ml) significantly decreased ROS level induced by LPS (Fig. 2B). The intensity of DCF-DA was decreased by ADR treatment (1, 10, and 50 μg/ml) in a dose-dependent manner, but ADR treatment at 1 μg/ml showed no significant decrease in the DCF-DA intensity (data not shown). NO level was also increased at 24 hr after LPS treatment, whereas LPS-induced NO level was decreased by ADR extract treatment (1, 10, and 50 μg/ml) in a dose-dependent manner (Fig. 2C).

ADR Extract Reduces ROS Production and Protein Nitration After SCI

ROS induces damage to such macromolecules as proteins, lipids, and DNA, resulting in functional impairments of these molecules (Valko et al., 2007). In particular, proteins are vulnerable to being carbonylated and nitrosylated on tyrosine residues by ROS (Berlett and Stadtman, 1997; le-Donne et al., 2006). Our data showed that ADR extract exhibited antioxidant effects in BV2 cells (see Fig. 2), so we hypothesized that ADR extract would alleviate ROS level after SCI. We determined the level of ROS after injury using a fluorescent dye, HEt, which is a specific indicator of superoxide anion ($O_2 \cdot^-$). Strong HEt fluorescence was observed in the cytoplasm of ventral horn motor neurons (VMN) and interneurons after injury (Fig. 3A). At higher magni-

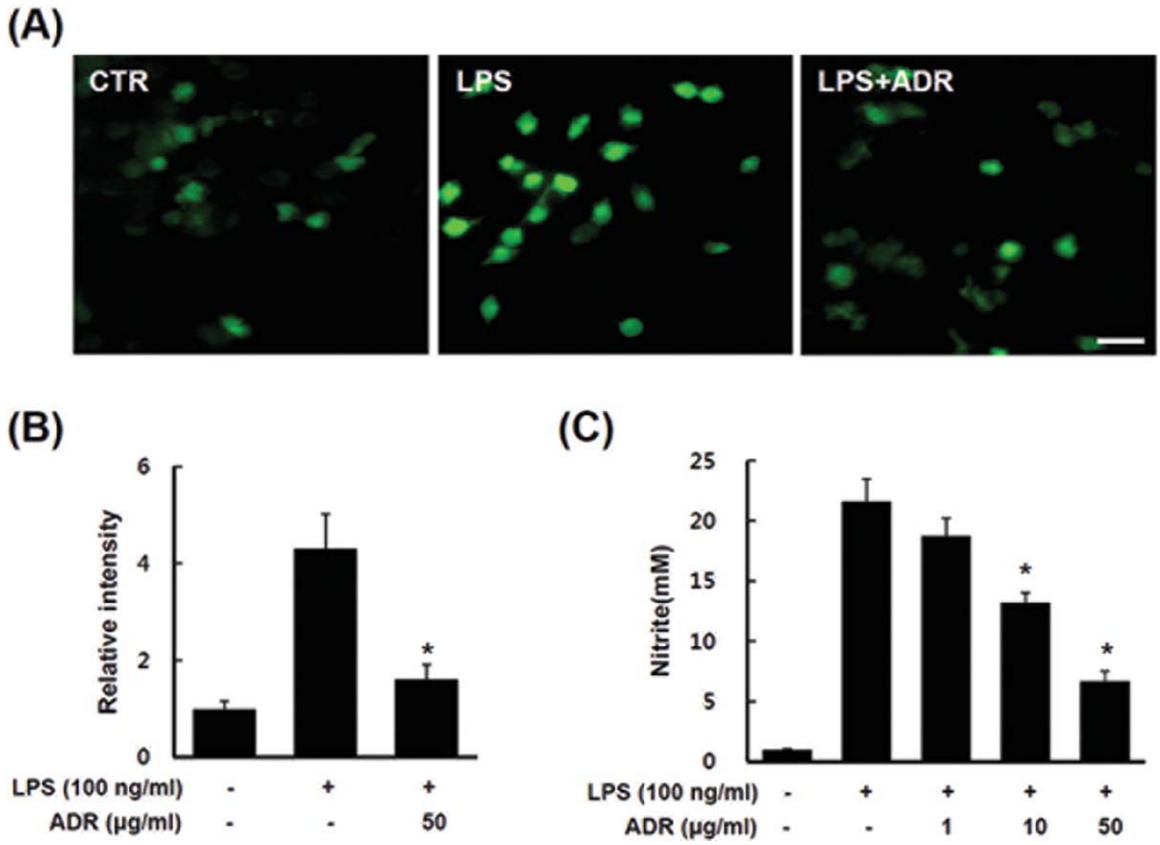

Fig. 2. ADR extract treatment inhibits ROS and NO production in LPS-activated BV2 cells. BV2 cells were seeded in 24-well plate (1×10^5 cells/well) and treated with ADR extract (50 μg/ml) 30 min before LPS (100 ng/ml) treatment. After 12 hr of incubation, DCF-DA (10 μM) was added, and the fluorescence was measured as described in Materials and Methods. **A,B:** DCF fluorescence in BV2 cells. **C:** NO production in BV2 cells at 24 hr after LPS treatment. The photographs are representative of results from three separate experiments, and data are mean ± SD. $^{\star}P < 0.05$ vs. LPS-treated control. Scale bar = 10 μm. [Color figure can be viewed in the online issue, which is available at wileyonlinelibrary.com.]

fication, trong HEt fluorescence in VMN appeared punctate in the cytoplasm (data not shown), as reported previously (Yune et al., 2008), suggesting the presence of $O_2{\cdot}^-$ in mitochondria (Sugawara et al., 2002). ADR extract (100 mg/kg) treatment decreased the number of HEt-positive VMN and the intensity of fluorescence in the spinal cord compared with the vehicle-treated cord (ADR extract 9.8 ± 1.1 vs. vehicle 16.5 ± 2.3 cells, $P < 0.05$; Fig. 3A). Quantitative analysis showed that the relative intensity of HEt fluorescence in the ADR extract-treated spinal cord was significantly lower than that in the vehicle-treated spinal cord at 4 hr after injury (Fig. 3B). Also, immunohistochemistry using an antinitrotyrosine antibody revealed some nitrotyrosine-positive neurons in the ventral horn of the injured spinal cord at 1 day after injury (Fig. 3C). ADR extract treatment markedly decreased the number of nitrotyrosine-positive neurons (Fig. 3C). Quantitative analysis showed that the number of nitrotyrosine-positive cells was significantly lower in the ADR extract-treated spinal cord than that in the vehicle-treated control at 4 hr after injury (ADR extract 23.2 ± 4.7 vs. vehicle 48.9 ± 8.6 cells, $P < 0.05$; Fig. 3D).

ADR Extract Inhibits Proinflammatory Factors Expression After SCI

Proinflammatory cytokines and mediators are increased in microglia after SCI, leading to neuronal and oligodendroglial cell death (Lee et al., 2003; Yune et al., 2007). Because ADR extract reduced LPS-induced inflammatory responses in microglial BV2 cells (see Fig. 1), we hypothesized that ADR extract would inhibit the expression of proinflammatory factors after SCI. Based on our previous report showing the temporal expression pattern of proinflammatory factors after SCI (Lee et al., 2004), the effect of ADR extract on the mRNA expression of proinflammatory cytokines and mediators at 4 hr after injury was examined. As shown in Figure 4A, TNF-α, IL-1β, IL-6, iNOS, and COX-2 mRNA expression were markedly increased after SCI as reported elsewhere (Lee et al., 2003; Yune et al., 2003). The protein levels of iNOS and COX-2 were also increased after injury (Fig. 4C). Furthermore, ADR extract treatment significantly alleviated the expression levels of proinflammatory cytokines and mediators compared with those of vehicle-treated control (Fig. 4B,D).

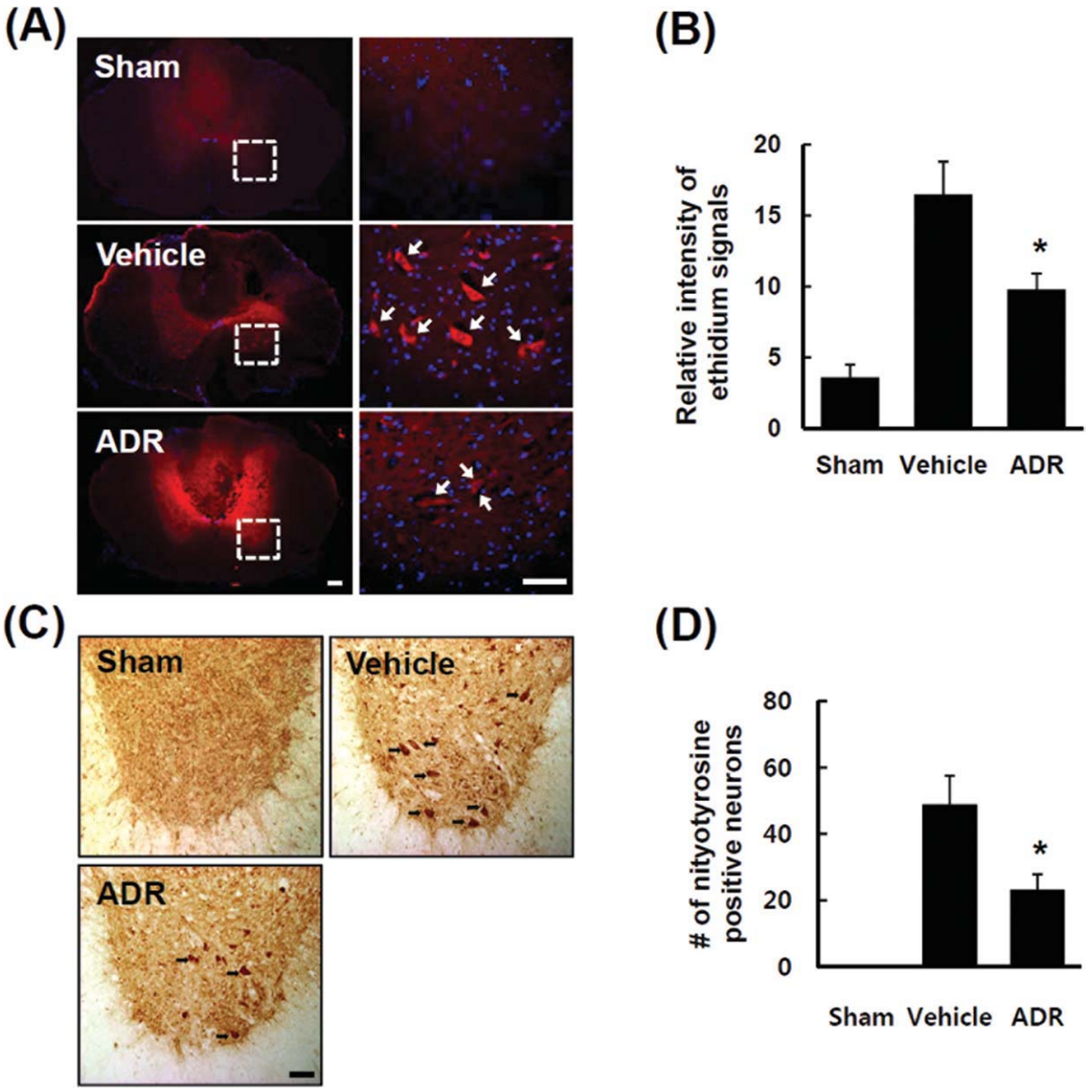

Fig. 3. ADR extract reduces superoxide anion production and protein nitration after SCI. Two hundred microliters of HEt (1 mg/ml in PBS) was injected i.v. 1 hr before the animals were killed, and spinal cord tissues were harvested at 4 hr after injury (n = 3/group). **A:** Representative photomicrographs of HEt fluorescence in the spinal cord. The right panel is a higher magnification of the ventral horn of spinal cord indicated by a boxed area in the left panel. Sections were taken 2 mm rostral to the lesion epicenter. **B:** Quantitative analysis of relative Etd fluoroscence intensity. The fluoroscence intensity was measured from spinal cord sections taken 2 mm rostral to the lesion epicenter. Data are mean ± SD obtained from three experiments. $\star P < 0.05$ vs. vehicle. **C:** Immunohistochemical staining of protein nitration in VMN 1 day after SCI. Coronal sections were taken 2 mm rostral to the lesion epicenter. **D:** For quantification, serial transverse sections (20 μm thickness) were collected every 500 μm from 2.5 mm rostral to 2.5 mm caudal to the lesion epicenter (total 11 sections), and nitrotyrosine-positive neurons (over 30 μm in diameter) were counted. $\star P < 0.05$ vs. vehicle. Scale bars = 30 μm in A; 50 μm in C. [Color figure can be viewed in the online issue, which is available at wileyonlinelibrary.com.]

ADR Extract Inhibits p38MAPK Activation and Pro-NGF Expression After SCI

It is known that p38MAPK mediates inflammatory responses in microglia (Bhat et al., 1998). Our previous report shows that oligodendroglial apoptosis is mediated by pro-NGF via p38MAPK activation in microglia after SCI (Yune et al., 2007). We demonstrated that ADR extract inhibited inflammatory responses after injury (see Fig. 4), so we hypothesized that ADR extract would inhibit p38MAPK activation and pro-NGF expression in microglia after SCI. As shown in Figure 5A, ADR extract treatment significantly decreased the level of p-

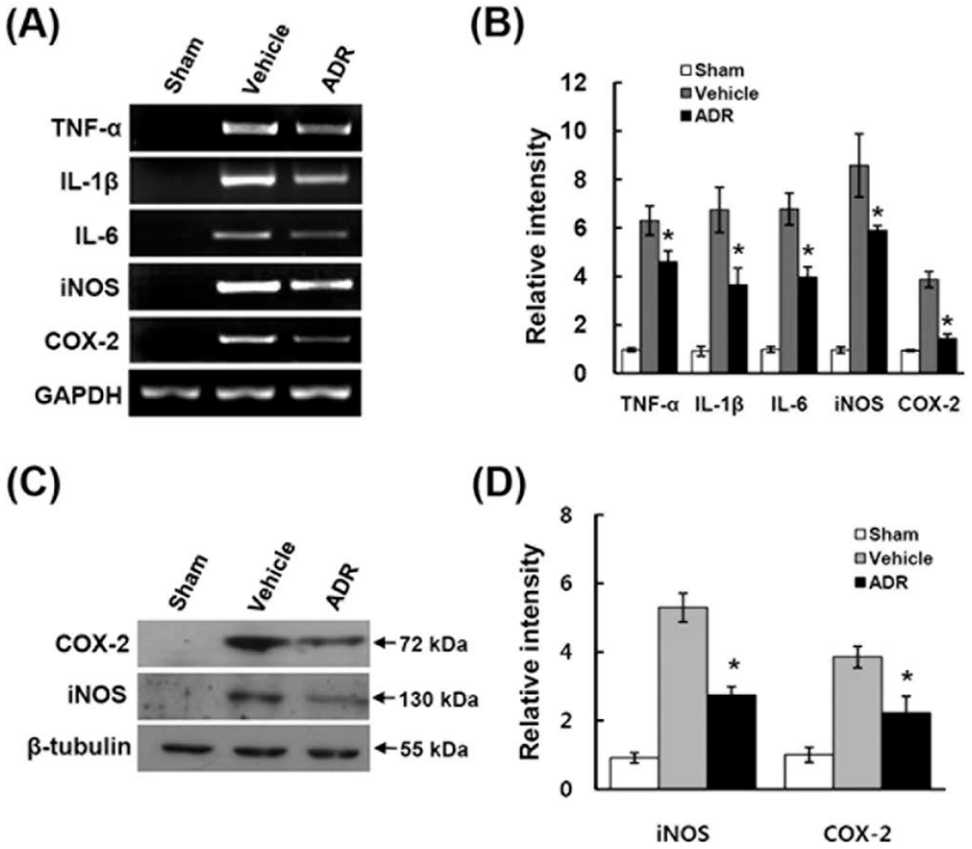

Fig. 4. ADR extract reduces proinflammatory cytokine and mediator expression after SCI. RNA isolation and total lysates from spinal cord samples at 4 or 24 hr after injury were processed as described in Materials and Methods (n = 3/group). **A:** RT-PCR of TNF-α, IL-1β, IL-6, iNOS, and COX-2 expression at 4 hr after SCI. **B:** Quantitative analysis of RT-PCR. Data represent mean ± SD from three separate experiments. $\star P < 0.05$ vs. vehicle. **C:** Western blots of proinflammatory mediators COX-2 and iNOS at 1 day after injury. **D:** Quantitative analysis of Western blots. Data are mean ± SD from three separate experiments. $\star P < 0.05$ vs. vehicle.

p38MAPK at 5 days after injury compared with vehicle control. Immunohistochemistry using an antibody against p-p38MAPK revealed p-p38MAPK in the intact spinal cord (Fig. 5B), but levels of signal were very low. After SCI, however, there was a marked increase in p-p38MAPK immunoreactivity (Fig. 5B). P-p38MAPK was colocalized to OX-42-positive microglia (Fig. 5C), as in a previous study (Yune et al., 2007). The majority of p-p38MAPK signal was observed in the GM; however, a small degree of p-p38MAPK signal was also observed within the WM. For quantification, p-p38MAPK-positive cells were counted for a predefined area of ventral horn. As shown in Figure 5C,D, the number of p-p38MAPK-positive microglia in the spinal cord was also markedly lower in the ADR extract-treated group compared with that in the vehicle-treated group (ADR extract 60.9 ± 7 vs. vehicle 101.5 ± 7 cells). In addition, immunohistochemistry with an antibody against OX-42 revealed that microglia exhibited an activated phenotype after SCI, including marked cellular hypertrophy and retraction of cytoplasmic processes (Fig. 5E, top) as reported by Hains and Waxman (2006). ADR extract treatment significantly decreased the proportion of activated microglia (determined by counting the number of cells with processes longer/shorter than the soma diameter) compared with control ($P < 0.01$; Fig. 5F). Furthermore, pro-NGF expression was significantly inhibited by ADR extract treatment compared with vehicle control (Fig. 5G). These data indicate that ADR extract inhibited microglial activation after SCI.

ADR Extract Inhibits Apoptotic Cell Death After SCI

Trauma to the spinal cord results in extensive apoptotic cell death of neurons and oligodendrocytes (Liu et al., 1997; Lee et al., 2003; Yune et al., 2007). Caspase-3 is also activated at an early stage of apoptotic cell death after SCI (Springer et al., 1999; Citron et al., 2000). Given the antiinflammatory and antioxidant effects of ADR extract in vitro and in vivo (see Fig. 1–4), we hypothesized that ADR extract would inhibit apoptotic cell death after SCI. Many TUNEL-positive cells were seen, mostly within the lesion area in the GM at 1 day (Fig. 6A, top) and mostly outside of the lesion area

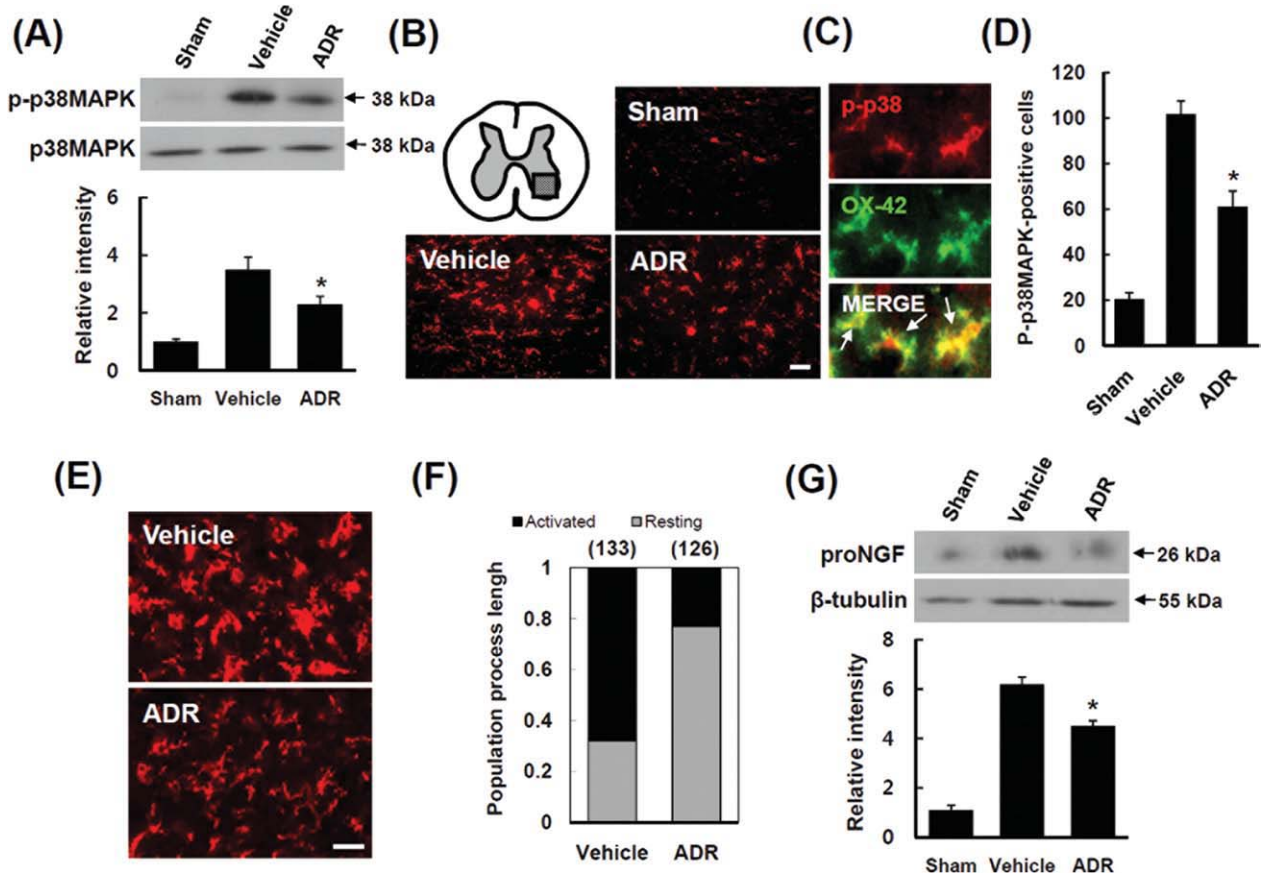

Fig. 5. ADR extract inhibits p38MAPK activation in microglia after SCI. **A:** Western blot of p-p38MAPK at 5 days after injury (top) and quantitative analysis of Western blots (bottom). ADR extract treatment significantly inhibited the p-p38MAPK level compared with that in vehicle control (bottom panel, n = 3/group). Values are mean ± SD of three separate experiments. $\star P < 0.05$ vs. vehicle. **B:** Presence of p-p38MAPK-positive microglia in the anterior horn of GM (indicated by a boxed area in the top panel) at 5 days after injury. Representative images are from sections 4 mm caudal to the lesion epicenter. **C:** OX-42-positive microglia were positive for p-p38MAPK (arrows) after SCI. **D:** Quantification revealed that, after SCI, there was a significant increase in the number of p-p38MAPK-positive cells compared with intact animals. Compared with the SCI group, ADR extract significantly reduced the number of p-p38MAPK-positive cells (n = 5/group). Values are mean ± SD of three separate experiments. $\star P < 0.05$ vs. vehicle. **E:** OX-42-positive microglia in the ventral horn at 5 days after injury. Sections were taken 2 mm caudal to the lesion epicenter. **F:** Quantification of the proportion of resting and activated microglia (n = 5/group). The number of resting or activated microglia in vehicle- or ADR extract-treated spinal cord was expressed as a percentage of total cells (100%) sampled. Data are means from five separate experiments. Parentheses indicate the number of microglia sampled. **G:** Western blot of pro-NGF expression at 5 days after injury (top) and quantitative analysis of Western blots (bottom, n = 3/group). Values are mean ± SD of three separate experiments. $\star P < 0.05$ vs. vehicle. Scale bars = 50 μm. [Color figure can be viewed in the online issue, which is available at wileyonlinelibrary.com.]

extending the entire length of the section (20 mm; Fig. 6B, bottom) in the WM at 5 days. Double labeling confirmed that most TUNEL-positive cells were neurons at 1 day and were oligodendrocytes at 5 days after injury, as previously reported (data not shown; Yune et al., 2009; Lee et al., 2010). As shown in Figure 6A,B, ADR extract (100 mg/kg) treatment significantly decreased the number of TUNEL-positive neurons and oligodendrocytes compared with the vehicle-treated control (neurons, ADR extract 152 ± 14 vs. vehicle 283 ± 35 cells; oligodendrocytes, ADR extract 48 ± 15 cells vs. vehicle 118 ± 17 cells, $P < 0.05$; Fig. 6B). Our previous studies showed that the level of cleaved (activated) forms of caspase-3 increased, peaking at 4 hr and 5 days after injury (Yune et al., 2007, 2008). ADR extract treatment significantly decreased the level of caspase-3 activation at 4 hr and 5 days after injury (Fig. 7A,B). Double labeling with antibodies against activated caspase-3 and CC1, an oligodendrocyte cell marker, also revealed that ADR extract treatment significantly reduced the number of activated caspase-3-positive oligodendrocytes in the WM at 5 days after injury compared with vehicle control (ADR extract 21 ± 11.2 vs. vehicle 43 ± 8.3 cells; Fig. 7C,D). Thus, our results indicate that ADR extract inhibits apoptotic cell death of neurons and oligodendrocytes after injury.

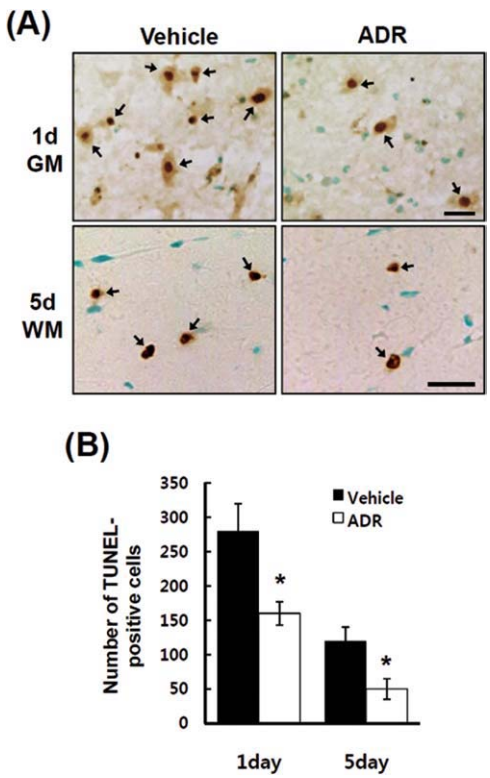

Fig. 6. Effect of ADR extract on apoptotic cell death of neurons and oligodendrocytes after SCI. Rats receiving spinal contusion injury were given ADR extract (100 mg/kg), beginning 2 hr after injury and then once per day. Spinal cord tissues from 1 or 5 days after injury were processed for TUNEL staining as described in Materials and Methods (n = 5/group). **A:** TUNEL-positive cells in the GM at 1 day after injury (top). Representative images were from the sections selected 1 mm rostral to the lesion epicenter. TUNEL-positive cells in the WM at 5 days after SCI (bottom). Representative images were from the sections selected 5 mm rostral to the lesion epicenter. **B:** Quantitative analysis of TUNEL-positive cells in the GM and the WM at 1 and 5 days after injury. Serial transverse sections (10 μm thickness) were collected every 100 μm from 2 mm rostral to 2 mm caudal to the lesion epicenter (total 40 sections for neurons) or 5 mm rostral to 5 mm caudal to the lesion epicenter (total 100 sections for oligodendrocytes). Data are mean ± SD obtained from five separate experiments. $^{**}P < 0.05$. Scale bar = 50 μm. [Color figure can be viewed in the online issue, which is available at wileyonlinelibrary.com.]

ADR Extract Improves Functional Recovery After SCI

Rats receiving an 25-mm weight-drop spinal injury were treated orally with ADR extract (100 mg/kg) beginning 2 hr after injury and then once daily for 14 consecutive days. Functional recovery was then evaluated for 5 weeks after injury using the BBB rating scale (Basso et al., 1995), inclined plane test (Rivlin and Tator, 1977), and footprint recordings (de Medinaceli et al., 1982; Stirling et al., 2004). The hindlimbs were paralyzed immediately after injury, and the rats recovered extensive movement of hindlimbs within 7–11 days after injury (Fig. 8A). ADR extract treatment after injury significantly increased the hindlimb locomotor function, as assessed by BBB scores, 14–35 days after injury compared with that observed in vehicle-treated control (35 days, ADR extract 11.3 ± 0.3 vs. vehicle 8.8 ± 0.5, $P < 0.001$; Fig. 8A). The angle of incline, determined 1–4 weeks after injury, was also significantly higher in ADR extract-treated rats compared with the vehicle control (4 weeks, ADR extract 59.8 ± 1.2 vs. vehicle 50.3 ± 3.7, $P < 0.05$; Fig. 8B). As shown in Figure 8C, footprint analyses for ADR extract-treated rats at 35 days after SCI disclosed fairly consistent forelimb–hindlimb coordination and very little toe dragging; these findings were comparable to those in the sham control animals. By contrast, the footprints obtained from vehicle-treated animals showed inconsistent coordination and extensive drags as revealed by ink streaks extending from both hindlimbs (Fig. 8C). With the 25-mm insult applied in the present study, hindpaws and central pads of control animals were not clearly recorded because of the hindlimb drags (Fig. 8C). Thus, we were unable to quantify footprint analysis using toe spread and ipsilateral distances (limb coordination).

ADR Extract Reduces Lesion Volume and Loss of Axon and Myelin After SCI

Traumatic injury to the spinal cord triggers immediate mechanical damage, followed by a secondary cascade of degenerative processes, leading to progressive tissue loss (Schwab and Bartholdi, 1996; Lee et al., 2003). To evaluate whether ADR extract reduces tissue loss after SCI, serial longitudinal sections from ADR extract- and vehicle-treated spinal cords were cut and stained with cresyl violet acetate. Extension of the cystic cavity in the lesion site was observed at 38 days after injury (Fig. 8D). The total lesion volume was significantly decreased upon ADR extract treatment compared with vehicle treatment (ADR extract 3.7 ± 0.99 vs. vehicle 8.3 ± 1.2 mm^3, $P < 0.05$; Fig. 8E). In addition, functional deficits after SCI were correlated with greater axon loss in the WM (Basso et al., 1996). To examine whether ADR extract preserves axons after injury, immunostaining with NF200 antibody was performed to detect the remaining axons, and the density of preserved axons was counted as described in Materials and Methods. In sham control animals, NF200-positive axons within the VST were dense, and axonal packing was uniform (Fig. 8F, sham). However, axon density was markedly decreased and exhibited a patchy distribution in injured tissue at 38 days after injury (Fig. 8F, vehicle). Quantitative analysis revealed that the number of NF200-positive axons in the VST was significantly higher in the ADR extract-treated group compared with the vehicle-treated group (2 mm, ADR extract 44% ± 3.3% vs. vehicle 29% ± 4%; 3 mm, ADR extract 65% ± 4.2% vs. vehicle 38% ± 4%, $P < 0.05$; Fig. 8G). Next, the extent of myelin loss after injury was assessed by Luxol fast blue staining. As shown in Figure 8H, extensive myelin loss near the lesion area was evident in

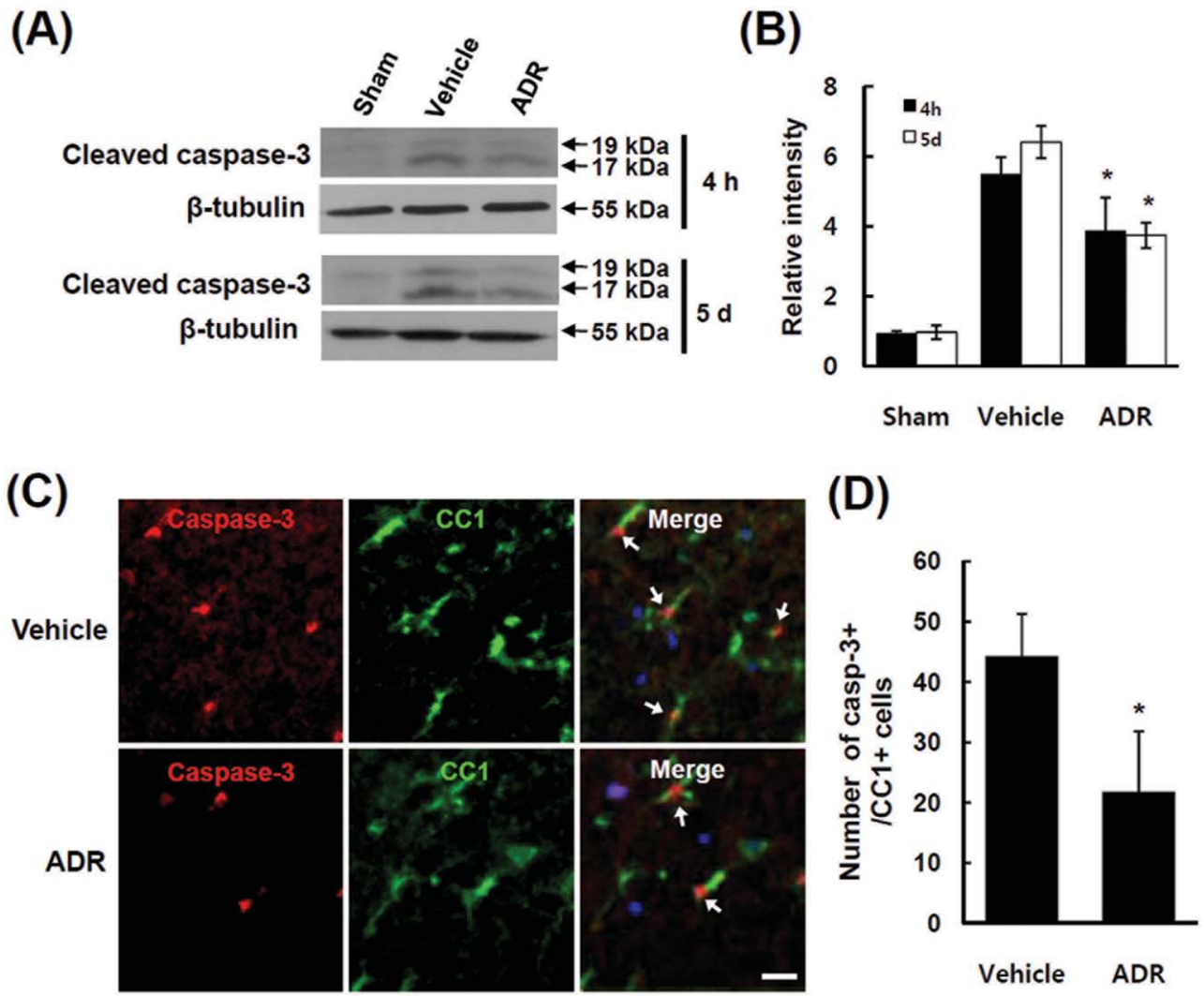

Fig. 7. ADR extract inhibits caspase-3 activation after SCI. **A:** Western blots of activated caspase-3 at 4 hr and 5 days after injury (n = 3/group). **B:** Quantitative analysis of Western blot. Data are mean ± SD of three separate experiments. $\star P < 0.05$ vs. vehicle control. **C:** Double labeling of cleaved caspase-3- and CC1-positive oligodendrocytes (arrows) in the WM at 5 days after SCI. Representative images were from the sections selected 2 mm rostral to the lesion epicenter. **D:** Quantification of capase-3 and CC1 double-positive oligodendrocytes in control and ADR extract-treated spinal cord at 5 days after injury as described in Materials and Methods. Serial transverse sections (10 μm thickness) were collected every 200 μm section from 4 mm rostral to 4 mm caudal to the lesion epicenter (total 40 sections). Data are mean ± SD from three separate experiments. $\star P < 0.05$. Scale bar = 20 μm. [Color figure can be viewed in the online issue, which is available at wileyonlinelibrary.com.]

the vehicle-treated group at 38 days after injury compared with the sham control (Fig. 8H, vehicle), whereas ADR extract treatment apparently attenuated myelin loss (Fig. 8H, ADR extract).

DISCUSSION

Here we examined the neuroprotective effect of ADR extract after SCI. Our results show that ADR extract decreased the levels of proinflammatory cytokines/mediators and ROS after injury. Furthermore, ADR extract reduced caspase-3 activation and apoptotic cell death of neurons and oligodendrocytes, thereby leading to enhanced functional recovery after injury. The involvement and/or contribution of proinflammatory cytokines and ROS in apoptotic cell death after SCI have been well documented (Bao and Liu, 2002; Lee et al., 2003; Yune et al., 2003, 2008). Thus, our data suggest that, after SCI, the neuroprotective effect of ADR extract may be attributed in part to its antiinflammatory and antioxidative effects.

After SCI, the recruitment of blood cells such as neutrophils and macrophages to the lesion site and the activation of resident microglia initiate and mediate acute inflammatory responses (Taoka and Okajima, 1998). For example, proinflammatory cytokines such as TNF-α, IL-

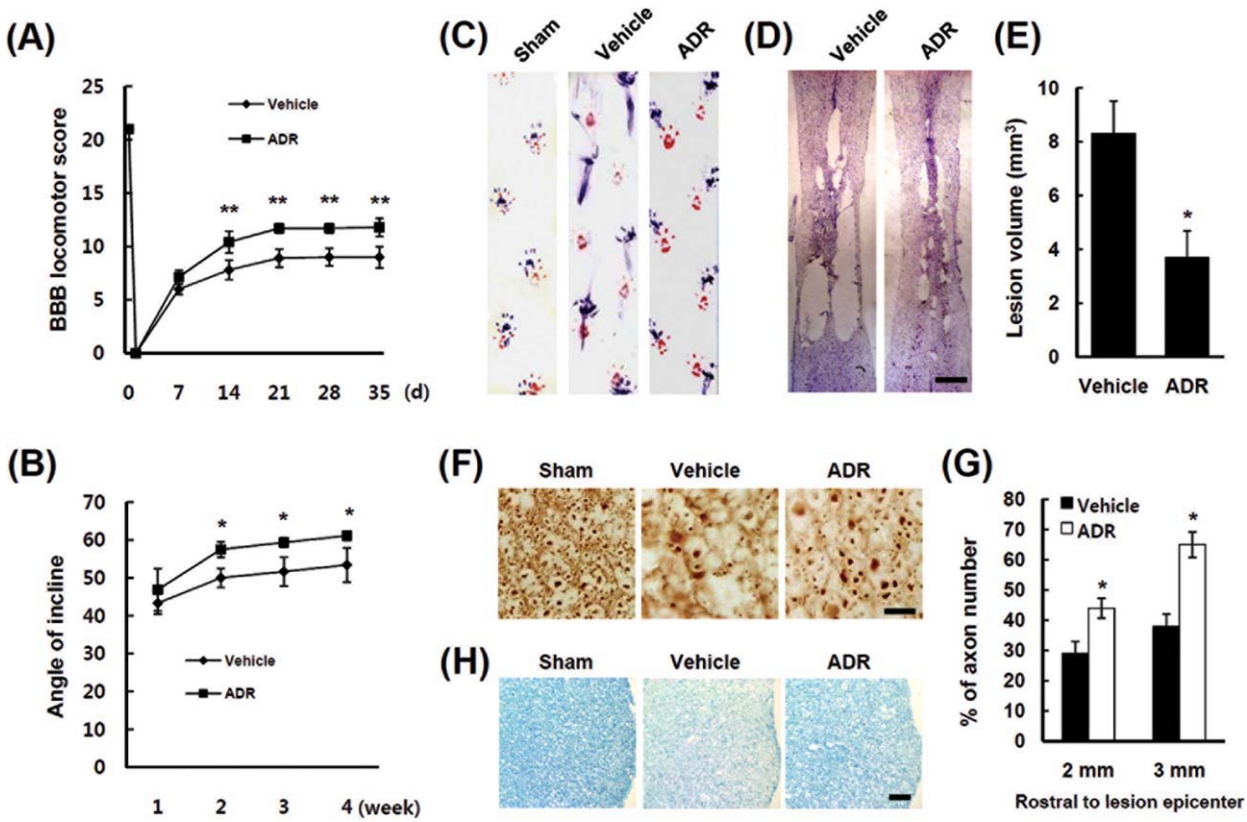

Fig. 8. ADR extract treatment improves functional recovery and reduces lesion volume and the loss of axon and myelin after SCI. After SCI, ADR extract was administered orally 2 hr after injury and then once per day for 2 weeks, and recovery was assessed via BBB, inclined plane test, and footprint analysis (n = 8/group). BBB scores (**A**) and inclined plane test (**B**) of vehicle- and ADR extract-treated groups after injury. $\star P < 0.05$, $\star\star P < 0.001$ vs. vehicle. **C:** Representative footprints obtained from each group at 37 days after SCI show that ADR extract-treated rats display fairly consistent weight-support plantar stepping and very little toe dragging. In contrast, vehicle control rats show consistent dorsal stepping and extensive toe dragging. **D:** Representative spinal cord tissues (1.2 mm from dorsal surface) showing cavitation in the lesion site at 38 days after injury. **E:** Quantitative analysis of lesion volumes at 38 days after injury (n = 5/group). Data are mean ± SD from five separate experiments. $\star P < 0.05$. **F:** Representative photographs of NF200-positive axons in sham-, vehicle-, and ADR extract-treated spinal sections 3 mm rostral to the lesion epicenter. **G:** Quantification of the remaining NF200-positive axons within preselected fields (40 × 40 μm, 1,600 μm^2) at specific sites within vestibulospinal tract (n = 5/group). Data are mean ± SD from five separate experiments. $\star P < 0.05$. **H:** Luxol fast blue staining shows that myelin loss in the lateral funiculus was extensive in the vehicle control compared with sham control after injury. ADR extract treatment decreased the extent of myelin loss after injury. Transverse sections were selected 2 mm rostral to the lesion site. Scale bars = 1 mm in D; 20 μm in F; 30 μm in H. [Color figure can be viewed in the online issue, which is available at wileyonlinelibrary.com.]

1β, and IL-6 and inflammatory mediators such as iNOS and COX-2 are rapidly up-regulated following SCI (Wang et al., 1996; Hayashi et al., 2000; Lee et al., 2000; Yune et al., 2003). Our previous reports also show that minocycline, an antiinflammatory drug, reduces apoptotic cell death and improves functional recovery by inhibiting the expression of proinflammatory cytokines and microglial activation after SCI (Lee et al., 2003; Yune et al., 2007). Thus, these observations indicate that the up-regulation of inflammatory factors in activated microglia plays a pivotal role in apoptotic cell death after SCI. Our data also show that ADR extract treatment decreased the levels of inflammatory factors such as TNF-α, IL-1β, IL-6, iNOS, and COX-2 in LPS-induced BV2 cells and the injured spinal cord (see Figs. 1, 4). Our results thus are in agreement with previous reports showing antiinflammatory effect of ADR extract in LPS-activated macrophages (Kang et al., 2007, 2008). Furthermore, our results show that ADR extract treatment inhibited p38MAPK activation and pro-NGF expression in microglia, which are known to be involved in oligodendroglial cell death after SCI (Yune et al., 2007), Therefore, our data indicate that the neuroprotective effects of ADR extract may be due to in part its antiinflammatory activity via inhibition of microglia activation after injury.

ROS play a critical role in the apoptotic cell death after SCI (Bao and Liu, 2002, 2004; Yune et al., 2008). After injury, apoptosis is triggered by the accumulation of free radicals such as superoxide anion ($O_2 \cdot^-$), hydroxyl radical, and peroxynitrite (Sugawara et al., 2002; Xu et al., 2005). Our study demonstrates that the level of

$O_2\cdot^-$ detected by Het dye is increased after SCI, and its level is decreased by ADR extract treatment (see Fig. 3A,B). Protein modifications such as protein carbonylation and nitration by free radicals and thereby protein dysfunction are generally accepted to be a major pathogenic mechanism of oxidative stress, and this phenomenon has been well studied in the injured spinal cord (Liu et al., 2000; Leski et al., 2001; Yune et al., 2008). After SCI, the level of NO has also been known to increase and to form peroxynitrite, a strong oxidant when it reacts with $O_2\cdot^-$ (Bao and Liu, 2002; Yune et al., 2003), which is known to mediate several destructive chemical reactions, including protein nitration (Liu et al., 2000; Yune et al., 2008). Our previous report demonstrates that protein nitrosylation increases at 1 day after SCI (Yune et al., 2008). Our data show that ADR extract treatment attenuated the number of protein nitrosylation-positive neurons after SCI (see Fig. 3C,D). Furthermore, a recent report shows that furanocoumarines such as 9-hydroxy-4-methoxypsoralen and alloimperatorin isolated from ADR extract, exert antioxidative activity against 2,2′-azobis(2-aminodinopropane)dihydrochloride (AAPH)-induced cellular damage in epithelial cells (Piao et al., 2004). Isoimperatorin and imperatorin from ADR extract are also known to exhibit antioxidative effects in macrophages (Abad et al., 2001). Based on these reports, these compounds present in ADR extract may partially contribute to their antioxidant effects after SCI, although we did not examine the antioxidative effect of active compounds isolated from ADR extract. Nevertheless, further studies on active compounds isolated from ADR extract in their antiinflammatory and/or antioxidative effects after SCI are needed.

Although herbal remedies are usually perceived as natural and thus devoid of side effects, they may contain such toxic materials as heavy metals (Bayly et al., 1995; Abbot et al., 1996). In our in vitro study, we found that ADR extract at concentrations ranging from 1 to 50 μg/ml exhibited no cytotoxicity (data not shown). Also, we showed that ADR extract (100 mg/kg) administered orally for 14 days provided the neuroprotective effects after SCI. However, no side effects were observed at this concentration of ADR extract throughout our in vivo experiments. Furthermore, we found that ADR extract at concentrations of 300 and 600 mg/kg showed no sign of side effects such as loss of body weight but exhibit the neuroprotective effect after SCI (data not shown).

In summary, we have investigated the neuroprotective effect of ADR extract as a potential therapeutic agent after SCI. Our results indicate that the inhibition of both proinflammatory factors and ROS by ADR extract may account in part for its neuroprotective effect. Our study thus suggests that ADR extract can be used as a candidate for an orally administered therapeutic agent for acute human SCI. Furthermore, the present study suggests that ADR extract could be utilized as a prodrug for use in the development of other novel neuroprotective agents for the treatment of neurodegenerative diseases such as Parkinson's disease, Alzheimer's disease, and amyotrophic lateral sclerosis and inflammatory disease such as multiple sclerosis.

REFERENCES

Abad MJ, de las HB, Silvan AM, Pascual R, Bermejo P, Rodriquez B, Villar AM. 2001. Effects of furocoumarins from *Cachrys trifida* on some macrophage functions. J Pharm Pharmacol 53:1163–1168.

Abbot NC, White AR, Ernst E. 1996. Complementary medicine. Nature 381:361.

Bao F, Liu D. 2002. Peroxynitrite generated in the rat spinal cord induces neuron death and neurological deficits. Neuroscience 115:839–849.

Bao F, Liu D. 2004. Hydroxyl radicals generated in the rat spinal cord at the level produced by impact injury induce cell death by necrosis and apoptosis: protection by a metalloporphyrin. Neuroscience 126:285–295.

Bareyre FM, Schwab ME. 2003. Inflammation, degeneration and regeneration in the injured spinal cord: insights from DNA microarrays. Trends Neurosci 26:555–563.

Basso DM, Beattie MS, Bresnahan JC. 1995. A sensitive and reliable locomotor rating scale for open field testing in rats. J Neurotrauma 12:1–21.

Basso DM, Beattie MS, Bresnahan JC, Anderson DK, Faden AI, Gruner JA, Holford TR, Hsu CY, Noble LJ, Nockels R, Perot PL, Salzman SK, Young W. 1996. MASCIS evaluation of open field locomotor scores: effects of experience and teamwork on reliability. Multicenter Animal Spinal Cord Injury Study. J Neurotrauma 13:343–359.

Bayly GR, Braithwaite RA, Sheehan TM, Dyer NH, Grimley C, Ferner RE. 1995. Lead poisoning from Asian traditional remedies in the West Midlands—report of a series of five cases. Hum Exp Toxicol 14:24–28.

Berlett BS, Stadtman ER. 1997. Protein oxidation in aging, disease, and oxidative stress. J Biol Chem 272:20313–20316.

Bhat NR, Zhang P, Lee JC, Hogan EL. 1998. Extracellular signal-regulated kinase and p38 subgroups of mitogen-activated protein kinases regulate inducible nitric oxide synthase and tumor necrosis factor-alpha gene expression in endotoxin-stimulated primary glial cultures. J Neurosci 18:1633–1641.

Blasi E, Barluzzi R, Bocchini V, Mazzolla R, Bistoni F. 1990. Immortalization of murine microglial cells by a v-raf/v-myc carrying retrovirus. J Neuroimmunol 27:229–237.

Block ML, Hong JS. 2005. Microglia and inflammation-mediated neurodegeneration: multiple triggers with a common mechanism. Prog Neurobiol 76:77–98.

Carter WO, Narayanan PK, Robinson JP. 1994. Intracellular hydrogen peroxide and superoxide anion detection in endothelial cells. J Leukoc Biol 55:253–258.

Chevallier A. 2001. Encyclopedia of medicinal plants. London: Dorling Kindersley Limited.

Citron BA, Arnold PM, Sebastian C, Qin F, Malladi S, Ameenuddin S, Landis ME, Festoff BW. 2000. Rapid upregulation of caspase-3 in rat spinal cord after injury: mRNA, protein, and cellular localization correlates with apoptotic cell death. Exp Neurol 166:213–226.

de Medinaceli L, Freed WJ, Wyatt RJ. 1982. An index of the functional condition of rat sciatic nerve based on measurements made from walking tracks. Exp Neurol 77:634–643.

Hains BC, Waxman SG. 2006. Activated microglia contribute to the maintenance of chronic pain after spinal cord injury. J Neurosci 26:4308–4317.

Hayashi M, Ueyama T, Nemoto K, Tamaki T, Senba E. 2000. Sequential mRNA expression for immediate early genes, cytokines, and neurotrophins in spinal cord injury. J Neurotrauma 17:203–218.

Hsu HY, Chen YP, Shen SJ, Hsu CC, Chang HC. 1986. Oriental materia medica: a concise guide. Long Beach, CA.45 p.

Kang OH, Lee GH, Choi HJ, Park PS, Chae HS, Jeong SI, Kim YC, Sohn DH, Park H, Lee JH, Kwon DY. 2007. Ethyl acetate extract

from *Angelica dahuricae radix* inhibits lipopolysaccharide-induced production of nitric oxide, prostaglandin E2 and tumor necrosis factor-alphavia mitogen-activated protein kinases and nuclear factor-kappaB in macrophages. Pharmacol Res 55:263–270.

Kang OH, Chae HS, Oh YC, Choi JG, Lee YS, Jang HJ, Kim JH, Kim YC, Sohn DH, Park H, Kwon DY. 2008. Anti-nociceptive and anti-inflammatory effects of *Angelicae dahuricae radix* through inhibition of the expression of inducible nitric oxide synthase and NO production. Am J Chin Med 36:913–928.

Ketai W, Huitao L, Xingguo C, Yunkun Z, Zhide H. 2001. Identification and determination of active components in *Angelica dahurica* Benth and its medicinal preparation by capillary electrophoresis. Talanta 54:753–761.

Kim CM, Heo MY, Kim HP, Sin KS, Pachaly P. 1991. Pharmacological activities of water extracts of Umbelliferae plants. Arch Pharm Res 14:87–92.

Kim SJ, Yune TY, Han CT, Kim YC, Oh YJ, Markelonis GJ, Oh TH. 2007. Mitochondrial isocitrate dehydrogenase protects human neuroblastoma SH-SY5Y cells against oxidative stress. J Neurosci Res 85:139–152.

Kim YO, Leem K, Park J, Lee P, Ahn DK, Lee BC, Park HK, Suk K, Kim SY, Kim H. 2001. Cytoprotective effect of *Scutellaria baicalensis* in CA1 hippocampal neurons of rats after global cerebral ischemia. J Ethnopharmacol 77:183–188.

Kondo T, Reaume AG, Huang TT, Carlson E, Murakami K, Chen SF, Hoffman EK, Scott RW, Epstein CJ, Chan PH. 1997. Reduction of CuZn-superoxide dismutase activity exacerbates neuronal cell injury and edema formation after transient focal cerebral ischemia. J Neurosci 17:4180–4189.

le-Donne I, Aldini G, Carini M, Colombo R, Rossi R, Milzani A. 2006. Protein carbonylation, cellular dysfunction, and disease progression. J Cell Mol Med 10:389–406.

Lee SM, Yune TY, Kim SJ, Park DW, Lee YK, Kim YC, Oh YJ, Markelonis GJ, Oh TH. 2003. Minocycline reduces cell death and improves functional recovery after traumatic spinal cord injury in the rat. J Neurotrauma 20:1017–1027.

Lee SM, Yune TY, Kim SJ, Kim YC, Oh YJ, Markelonis GJ, Oh TH. 2004. Minocycline inhibits apoptotic cell death via attenuation of TNF-alpha expression following iNOS/NO induction by lipopolysaccharide in neuron/glia co-cultures. J Neurochem 91:568–578.

Lee YB, Yune TY, Baik SY, Shin YH, Du S, Rhim H, Lee EB, Kim YC, Shin ML, Markelonis GJ, Oh TH. 2000. Role of tumor necrosis factor-alpha in neuronal and glial apoptosis after spinal cord injury. Exp Neurol 166:190–195.

Leski ML, Bao F, Wu L, Qian H, Sun D, Liu D. 2001. Protein and DNA oxidation in spinal injury: neurofilaments—an oxidation target. Free Radic Biol Med 30:613–624.

Liu D, Ling X, Wen J, Liu J. 2000. The role of reactive nitrogen species in secondary spinal cord injury: formation of nitric oxide, peroxynitrite, and nitrated protein. J Neurochem 75:2144–2154.

Liu XZ, Xu XM, Hu R, Du C, Zhang SX, McDonald JW, Dong HX, Wu YJ, Fan GS, Jacquin MF, Hsu CY, Choi DW. 1997. Neuronal and glial apoptosis after traumatic spinal cord injury. J Neurosci 17:5395–5406.

Min KJ, Jou I, Joe E. 2003. Plasminogen-induced IL-1beta and TNF-alpha production in microglia is regulated by reactive oxygen species. Biochem Biophys Res Commun 312:969–974.

Min KJ, Pyo HK, Yang MS, Ji KA, Jou I, Joe EH. 2004. Gangliosides activate microglia via protein kinase C and NADPH oxidase. Glia 48:197–206.

Okamoto T, Yoshida S, Kobayashi T, Okabe S. 2001. Inhibition of concanavalin A-induced mice hepatitis by coumarin derivatives. Jpn J Pharmacol 85:95–97.

Park AY, Park SY, Lee J, Jung M, Kim J, Kang SS, Youm JR, Han SB. 2009. Simultaneous determination of five coumarins in *Angelicae dahuricae radix* by HPLC/UV and LC-ESI-MS/MS. Biomed Chromatogr 23:1034–1043.

Perry LM. 1980. Medicinal plants of East and Southeast Asia: attributed properties and uses. Cambridge, MA: The MIT Press.411 p.

Piao XL, Park IH, Baek SH, Kim HY, Park MK, Park JH. 2004. Antioxidative activity of furanocoumarins isolated from *Angelicae dahuricae*. J Ethnopharmacol 93:243–246.

Qin L, Liu Y, Wang T, Wei SJ, Block ML, Wilson B, Liu B, Hong JS. 2004. NADPH oxidase mediates lipopolysaccharide-induced neurotoxicity and proinflammatory gene expression in activated microglia. J Biol Chem 279:1415–1421.

Rivlin AS, Tator CH. 1977. Objective clinical assessment of motor function after experimental spinal cord injury in the rat. J Neurosurg 47:577–581.

Saiki Y, Morinaga K, Okegawa O, Sakai S, Amaya Y. 1971. [On the coumarins of the roots of *Angelica dahurica* Benth et Hook]. Yakugaku Zasshi 91:1313–1317.

Schwab ME, Bartholdi D. 1996. Degeneration and regeneration of axons in the lesioned spinal cord. Physiol Rev 76:319–370.

Springer JE, Azbill RD, Knapp PE. 1999. Activation of the caspase-3 apoptotic cascade in traumatic spinal cord injury. Nat Med 5:943–946.

Stirling DP, Khodarahmi K, Liu J, McPhail LT, McBride CB, Steeves JD, Ramer MS, Tetzlaff W. 2004. Minocycline treatment reduces delayed oligodendrocyte death, attenuates axonal dieback, and improves functional outcome after spinal cord injury. J Neurosci 24:2182–2190.

Sugawara T, Lewen A, Gasche Y, Yu F, Chan PH. 2002. Overexpression of SOD1 protects vulnerable motor neurons after spinal cord injury by attenuating mitochondrial cytochrome c release. FASEB J 16:1997–1999.

Taoka Y, Okajima K. 1998. Spinal cord injury in the rat. Prog Neurobiol 56:341–358.

Valko M, Leibfritz D, Moncol J, Cronin MT, Mazur M, Telser J. 2007. Free radicals and antioxidants in normal physiological functions and human disease. Int J Biochem Cell Biol 39:44–84.

Wang CX, Nuttin B, Heremans H, Dom R, Gybels J. 1996. Production of tumor necrosis factor in spinal cord following traumatic injury in rats. J Neuroimmunol 69:151–156.

Wanger H. 1999. Arzneidrogen und ihre Inhaltsstoffe. Pharmazeutische Biologie Band 2. Stuttgart: Wissenschaftliche Verlagsgesellschaft.

Xu W, Chi L, Xu R, Ke Y, Luo C, Cai J, Qiu M, Gozal D, Liu R. 2005. Increased production of reactive oxygen species contributes to motor neuron death in a compression mouse model of spinal cord injury. Spinal Cord 43:204–213.

Yune TY, Chang MJ, Kim SJ, Lee YB, Shin SW, Rhim H, Kim YC, Shin ML, Oh YJ, Han CT, Markelonis GJ, Oh TH. 2003. Increased production of tumor necrosis factor-alpha induces apoptosis after traumatic spinal cord injury in rats. J Neurotrauma 20:207–219.

Yune TY, Lee SM, Kim SJ, Park HK, Oh YJ, Kim YC, Markelonis GJ, Oh TH. 2004. Manganese superoxide dismutase induced by TNF-beta is regulated transcriptionally by NF-kappaB after spinal cord injury in rats. J Neurotrauma 21:1778–1794.

Yune TY, Lee JY, Jung GY, Kim SJ, Jiang MH, Kim YC, Oh YJ, Markelonis GJ, Oh TH. 2007. Minocycline alleviates death of oligodendrocytes by inhibiting pro-nerve growth factor production in microglia after spinal cord injury. J Neurosci 27:7751–7761.

Yune TY, Lee JY, Jiang MH, Kim DW, Choi SY, Oh TH. 2008. Systemic administration of PEP-1-SOD1 fusion protein improves functional recovery by inhibition of neuronal cell death after spinal cord injury. Free Radic Biol Med 45:1190–1200.

Yune TY, Lee JY, Cui CM, Kim HC, Oh TH. 2009. Neuroprotective effect of Scutellaria baicalensis on spinal cord injury in rats. J Neurochem 110:1276–1287.